Close pairs recognition and suppression

Munich, 23rd October 2007

Martin Jurkovič

1 Introduction

This document reports on investigations focused on RICH signatures of close pairs (CP) and suggests a possibility to suppress the CP significantly while keeping as much signal as possible. For the investigations only the signal of the RICH detector and inner MDC was used (these two detectors are placed before the magnetic field).

In a heavy ion reaction conversion is the dominant source of e^+/e^- pairs with small opening angle and low momenta single tracks. These tracks are normally bent out of the detector acceptance by the magnetic field, but produce a lot of hits in the detectors before the magnetic field (RICH, inner MDC). In a high multiplicity environment these hits can significantly contribute in several ways to the combinatorial background. Therefore a successful identification of the CP signal is crucial for fake and background reduction.

For this analysis the ArKCl simulation PLUTO GEN2 has been used. From all events only events with primary e^+/e^- track multiplicity **M=2** have been selected. In addition both tracks are requested to originate from the same source and to produce a signal in the RICH detector and inner MDC. This selection is sufficient as long as the signature of a close pair compared to the one of a single track is the subject of interests.

The analysis is based on the PidTrackCand category, which adds additional requirement on the tracks.The track segments before the magnetic field have to be combined with track segments behind the magnetic field.

The input sample is divided into two categories:

1. **double-track rings**: both partners of the pair contribute to a single identified ring. Cases, where two identified rings have a common region are excluded. This sample corresponds to close pair selection.

2. **single-track rings**: both partners of the pair build a well defined, separated and identified ring with absolutely **NO overlap**. This sample corresponds to open pairs with opening angle of at least 5^o.

2 Properties of selected tracks

From all together 2.5 million input events, 1.8 million events have been used for the analysis containing 205,273 reconstructed primary pairs (in this document reconstructed pair does not correspond to the HYDRA pair framework reconstruction). The yields of the dominant electron sources are summarized in Tab. 1.

Table 1: Yields of the e^+/e^- sources.

Process	Generator Info	Pairs
γ–conversion from π^0	7001	**90,766**
π^0 Dalitz	7051	**38,462**
η Dalitz	17051	**37,912**
Δ Dalitz	34051	**37,798**

In Fig. 1 the true e^+/e^-–pair opening angle distribution for the dominant sources is depicted. The displayed range is restricted to an opening angle range $0^o \leq \Theta_{OP} \leq 25^o$,

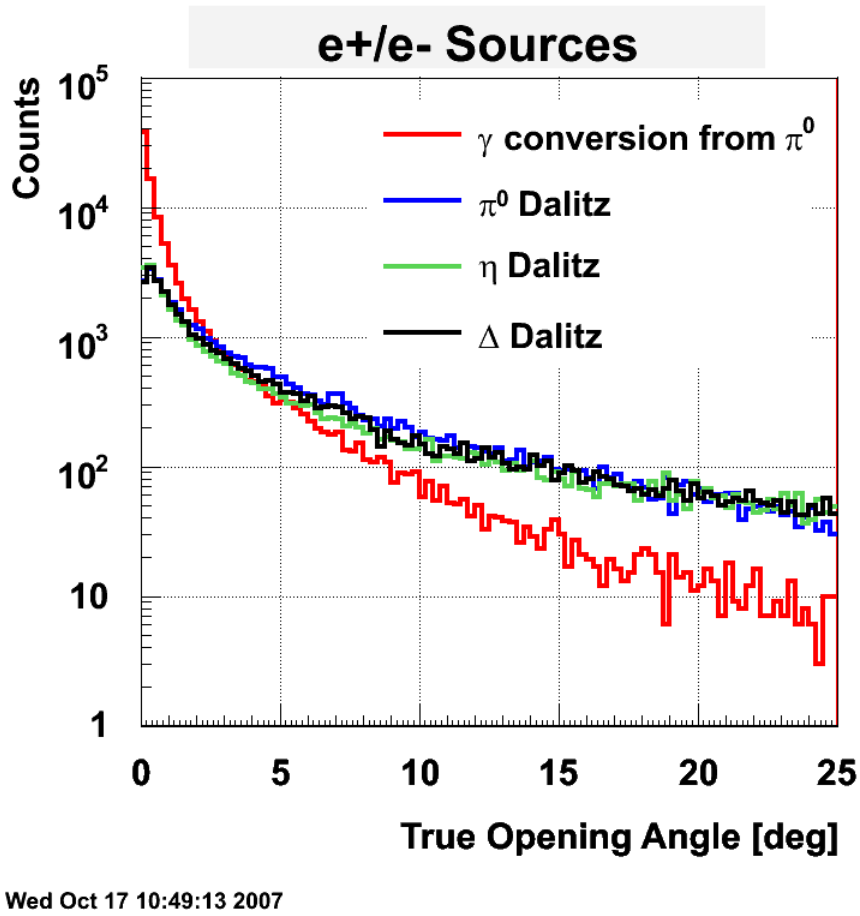

Figure 1: e^+/e^-–pair opening angle distribution for different sources. Conversion dominates at angles below 2^o.

which corresponds to the range used in the HYDRA analysis for the inner MDC (*angle to closest lepton candidate*).

The comparison of the true opening angle (left) distribution and the distribution of the *angle to the closest lepton candidate* (right) as measured by the inner MDC is shown in Fig. 2. The distributions are plotted for single- and double- track rings for all sources. For the shaded spectra, an additional minimum momentum p>50 MeV/c for both legs of the pair was required.

In Tab. 2 the influence of the momentum cut on the yields is shown. Since the HADES spectrometer was designed to identify charged particle momenta above 50 MeV/c, particles with smaller momenta might induce measurable signal in the detectors. The comparison is made only here and the momentum cut is not used in further investigations.

Table 2: Dependence of particle yields on momenta.

Ring type	All pairs	After momentum cut
Double track rings	139,109	128,617
Single track rings	26,633	20,603

True momentum distributions of double- and single- track rings are displayed in Fig. 3.

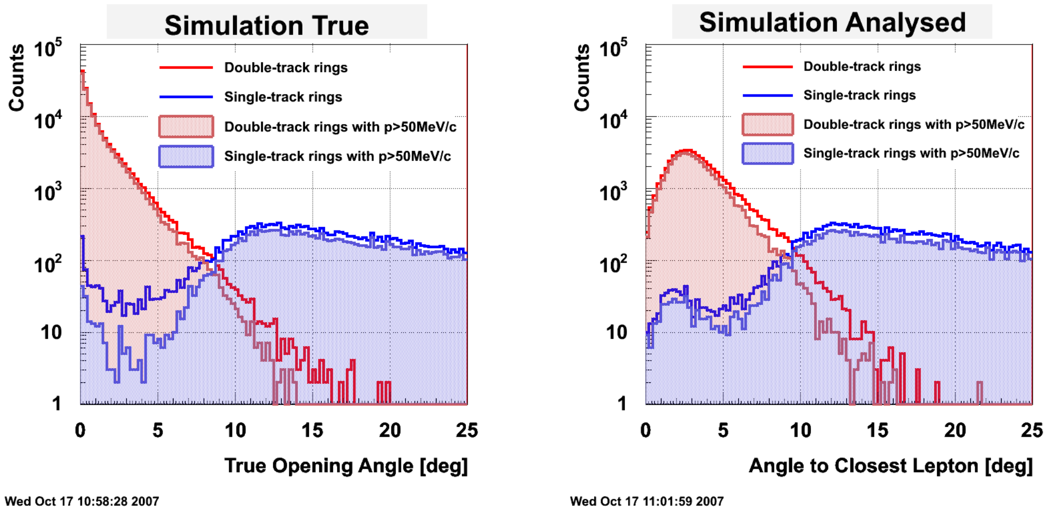

Figure 2: **Left:** True opening angle distribution for single- and double- track rings. **Right:** Reconstructed angle to closest lepton track for single- and double- track rings

The black lines highlight the true momenta p=50 MeV/c for both partners of the pair. From these figures it can be deduced, that low momentum electron tracks can be successfully digitized and identified before the magnetic field.

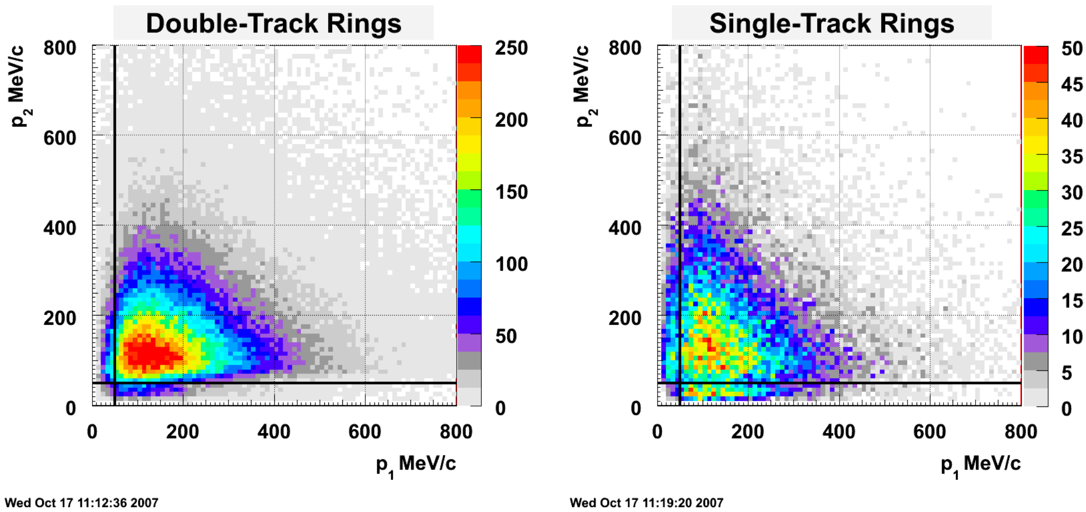

Figure 3: **Left:** True momentum distribution for double-track rings. **Right:** True momentum distribution for single-track rings.

In Fig. 4 the comparison of the *angle to the closest lepton candidate* distribution for both legs of the pair for the single- and double-track rings is made. The yields show identical values in 86% of all cases for double-track rings and in 93% for single-track rings. The disagreement is visible mainly at small angles, even for cases, when both partners are in different MDC cells. This may be explained by the presence of a third track close to the pair under investigation or by the presence of a ghost. In both cases the angle is then calculated to the “third partner”.

In Fig. 5 the inner MDC (MDC0) χ^2 distribution for both legs of the pair is depicted. A strong χ^2 correlation can be observed, which means, that the pair shares the same MDC0

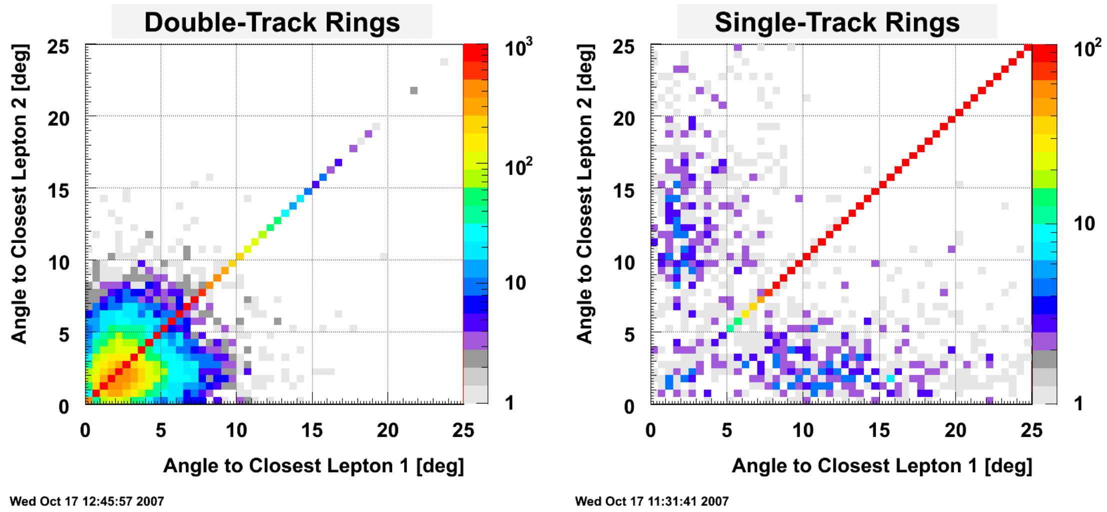

Figure 4: **Left:** Angle to closest lepton candidate for double-track rings. **Right:** Angle to closest lepton candidate for single-track rings.

segment. For double-track rings this happens in 63% of all cases, while for single-track rings altogether only 40 cases can be found in the input sample. Among these same MDC0 segment candidates 49% of the segments are unfitted for double-track rings, while for single-track rings all 40 segments are unfitted. This means, that 31% of pairs, which share the same ring in RICH and the same segment in MDC are propagated in the analysis as a single track and contribute only to the combinatorial background or produce fake combinations.

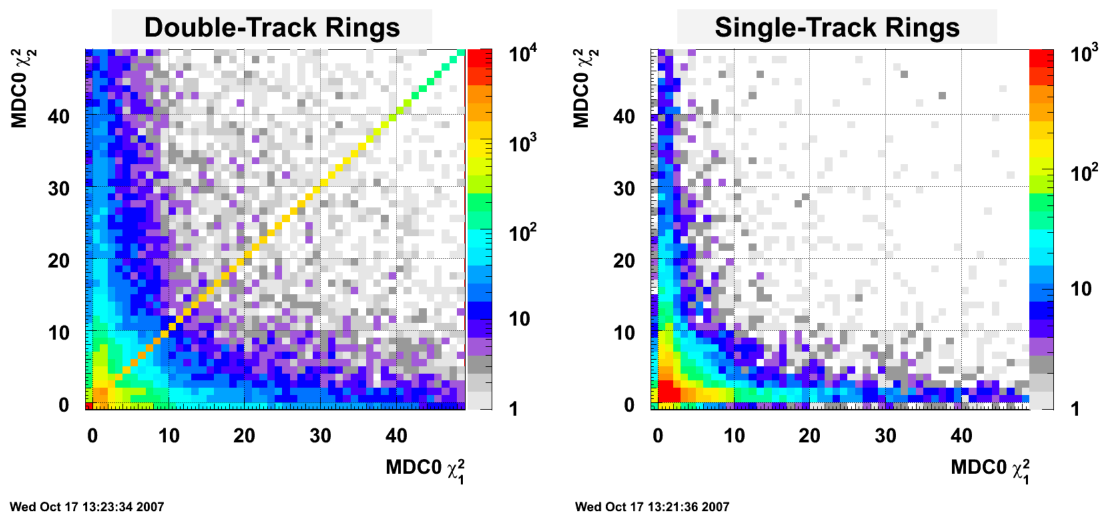

Figure 5: **Left:** MDC0 χ^2 distribution for both legs of the pair for double-track rings. **Right:** MDC0 χ^2 distribution for both legs of the pair for single-track rings.

A minor contribution to the combinatorial background occurs, when only one leg of the pair is fitted in the MDC0, the second is unfitted. For double-track rings this situation happens in 8%, for single-track rings in 4% of all cases for the corresponding yield in the sample. In total there are 56,175 close pairs, which are unrecognized by the inner MDC and contribute to a single ring in RICH. The numbers are summarized in Tab. **??** and the true opening angle distributions for the above mentioned cases are shown in Fig. 6.

Table 3: Yields for different quality of the MDC0 segment fit for close and open pairs.

Ring category	total	same χ^2	same unfitted χ^2	one leg unfitted
double-track rings	139,109	87,987	42,725	10,913
single-track rings	26,633	40	40	1,192

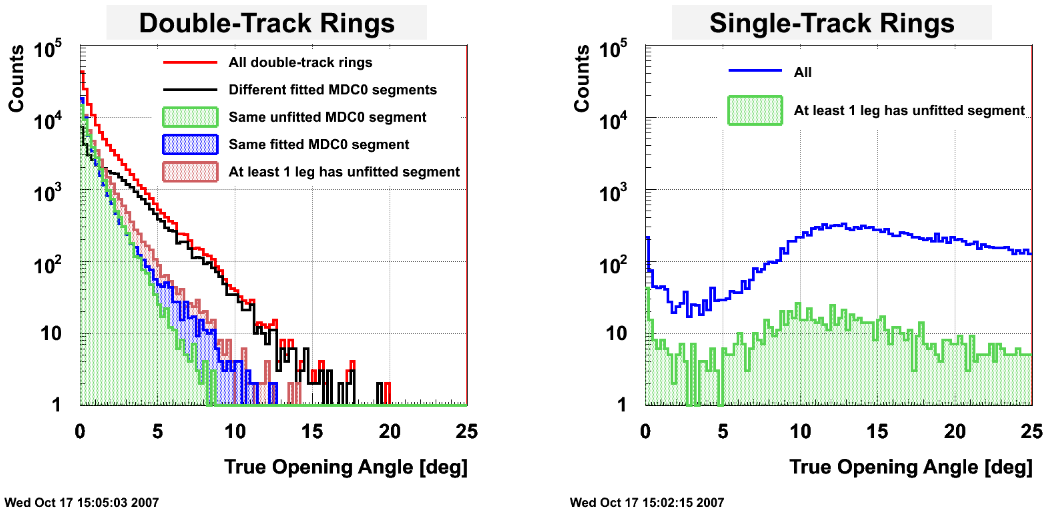

Figure 6: **Left:** True opening angle distribution for double-track rings for different MDC0 segment properties. **Right:** True opening angle distribution for single-track rings for different MDC0 segment properties.

For single-track rings there is a good agreement in the pair opening angle reconstructed from RICH and MDC0 coordinates (Fig. 7). In the case of double-track rings the opening angle can not be reconstructed in RICH (from definition it is the same ring), it can be reconstructed only for some cases in the MDC0 (if the two tracks do not share the same segment) as it is shown in Fig.8. A correlation between the opening angles reconstructed in the MDC0 and true opening angles for close pairs, which cannot be recognized by only χ^2 cut is shown on the left side. The same correlation for close pairs, which can be recognized via negative value of χ^2 for both legs or via a reconstructed small angle, is shown on the right side.

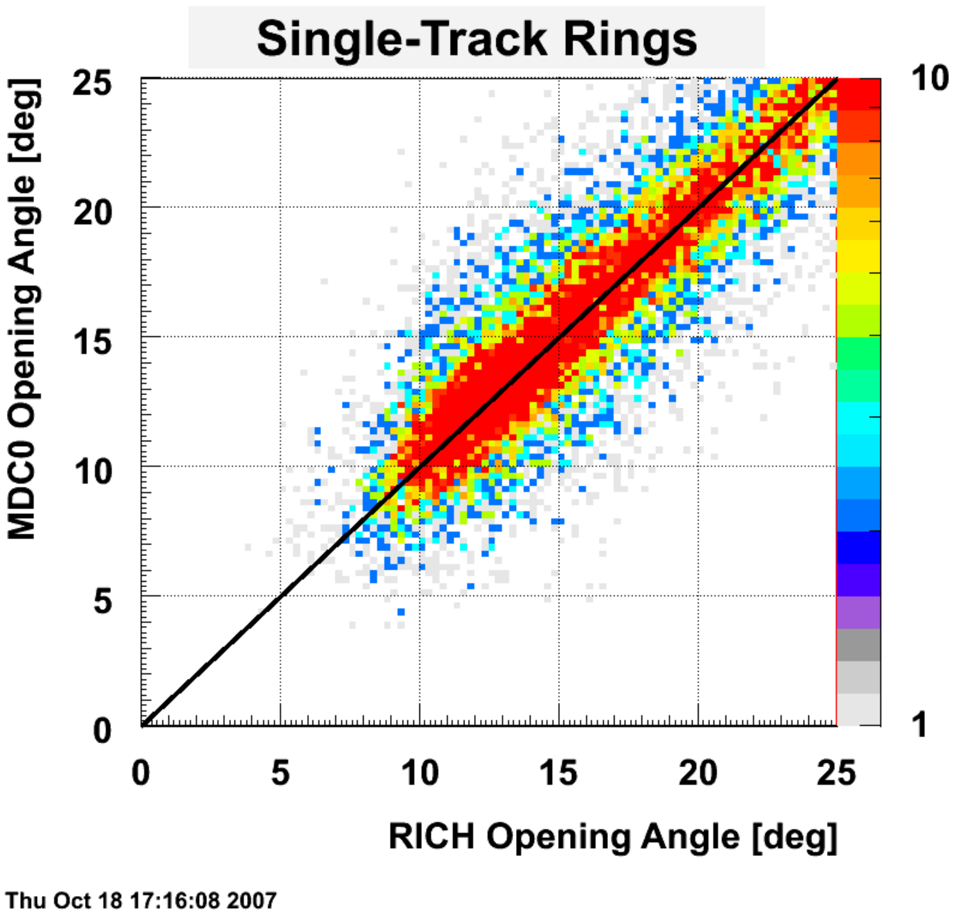

Figure 7: Comparison of reconstructed opening angles in RICH and MDC0.

3 RICH signal

In Fig. 9 the RICH ring properties

- pattern matrix (PM)
- average charge (AV_charge)
- number of pads (npads)
- ring centroid (centroid)

are displayed against each other for double- (left) and single- (right) track rings without any additional cut on the quality of the track for inner MDC segments.

Comparing the distributions only little differences can be observed. The most promising candidates for close pair recognition are the *pattern matrix* and the *number of pads* distributions. Since these two distributions are correlated, the *number of pads* distribution was chosen (Fig 10) for the further investigations. Number of pads building a single-track ring is plotted in blue, the double-track ring distribution is plotted in red. The brown-shaded spectrum is plotted for double-track rings with additional condition on MDC0 segment fit quality. The cut should select close pairs unresolved by the MDC0 (same fitted segment or segment from one leg is unfitted). The larger average number of pads indicates the presence of twice as many photons as expected for a single e^+/e^- track. The black lines in the histogram represent possible cuts on *number of pads* to suppress these close pairs. The yields as a function of the cut are summarized in Tab. 4.

Table 4: Open pair and close pair yields for different number of pads cuts.

Ring category	Total	npads<20	npads<25	npads<30
double-track rings	139,102	27.2%	48.8%	70.0%
double-track rings (unrecognized close pairs)	56,175	27.2%	47.7%	69.1%
single-track rings	26,633	65.0%	86.3%	95.9%

4 Conclusion

As it was shown in the previous sections, not all segments originating from close pairs are identified in the inner MDC. The cut on good segment fit is not sufficient enough and **∼1/3** of the close pairs are identified as good single tracks. It was shown, that using additional information from the RICH signal can improve the situation. How many of the close pairs can be suppressed, depends on the chosen cut. All investigations have been done on simulation data, the last word has to come from experiment.

Rejecting all rings with more than **25 pads** would reduce the number of previously **unrecognized close pair induced single tracks** by about a factor **2** while the true single tracks (**signal**) are reduced only by **14%**.

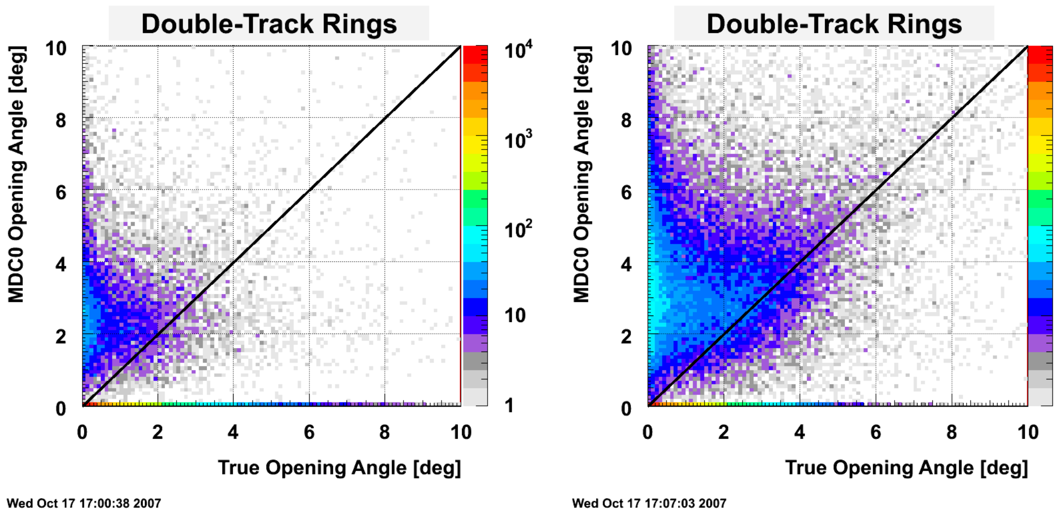

Figure 8: **Left:** Comparison of reconstructed opening angles in MDC0to true opening angles for unrecognized close pairs. **Right:** Comparison of reconstructed opening angle in MDC0 to true opening angles for close pairs, which can be recognized.

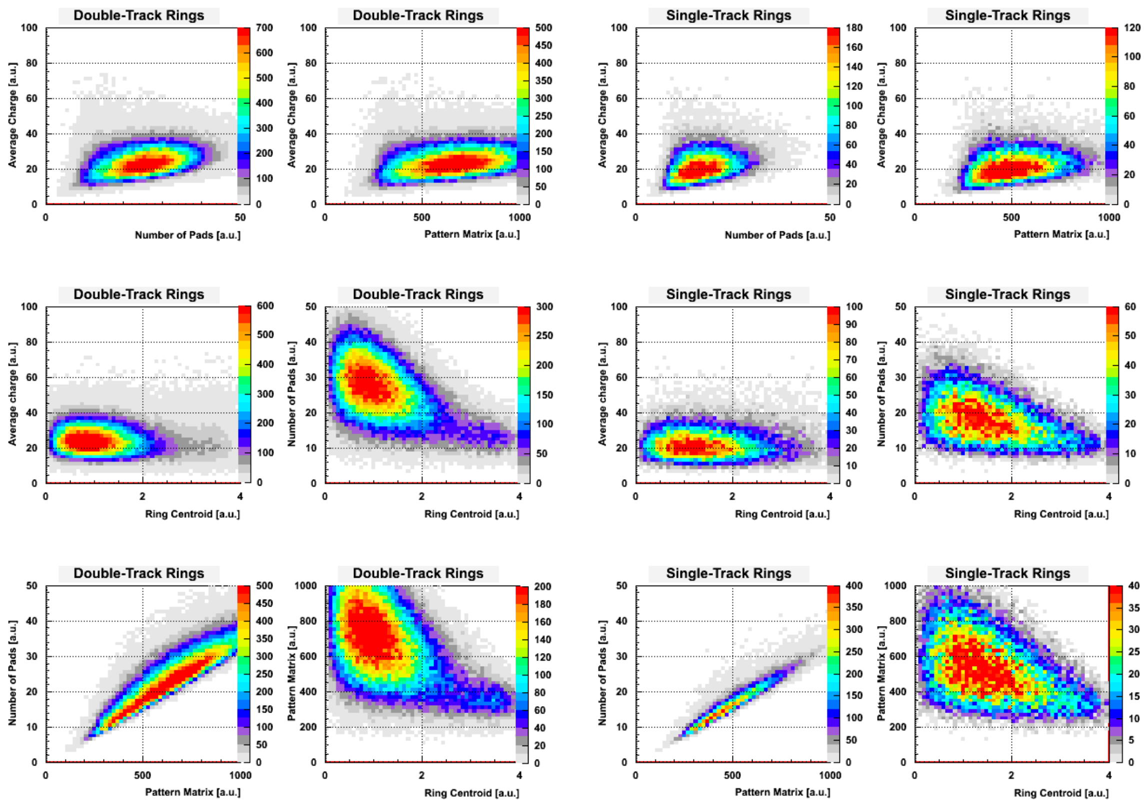

Figure 9: **Left:** Ring properties for double-track rings. **Right:** Ring properties for single-track rings.

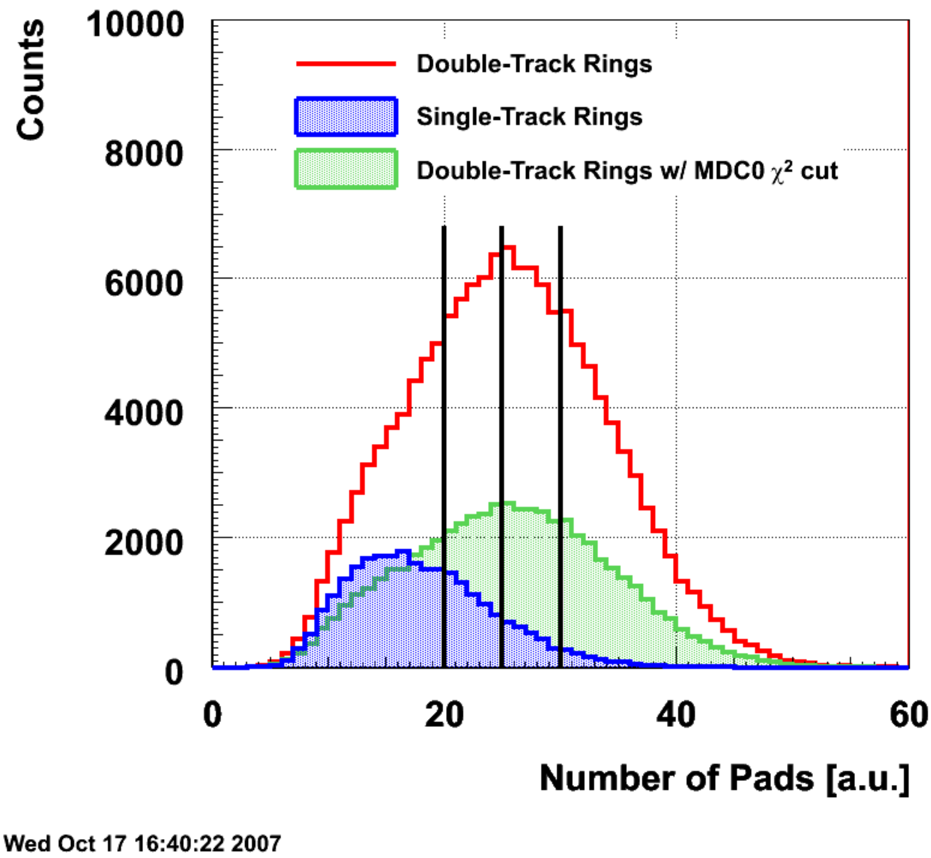

Figure 10: Number of pads for single- (blue), double- (red) and double-track ring which are unrecognized by MDC0 as close pairs.